Power Transformer Faults: Analysis, Classification and Protection

VIKRAMSINGH R. PARIHAR[1], ROSHANI S. NAGE[1], HARSHADA M. RAGHUWANSHI[2], MOHINI G. FUSE[3], DR. SONI A. CHATURVEDI4[4]

[1]Department of Electrical Engineering, Prof Ram Meghe College of Engineering and Management, Badnera-Amravati, INDIA
[2]Department of Computer Engineering, Trinity College of Engineering and Research, Pune, INDIA
[3]Department of Electrical Engineering, Ballarpur Institute of Technology, Ballarpur, Chandrapur, INDIA
[4]Department of Electronics & Communication Engineering, Priyadarshini College of Engineering, Nagpur, INDIA

Abstract: - With the increase in power consumption, the safety of the power transformers has increased manifolds. Ideally, there should be a no-fault operation of power transformer which is yet to be achieved. The objective of this paper is to provide a complete protection scheme of power transformers. The faults are analysed and classified using Discrete Fourier Transform (DFT) and Wavelet Transform. The DFT based controller is used to detect inrush and fault currents. We have used wavelet transform and it has proven to be a very effective tool for detailed analysis of these transients. In addition, Fuzzy logic controller, with minimal computational complexity, is implemented for the differentiation of inrush, internal and external faults using the detailed coefficients obtained by wavelet analysis providing successful classification. On the basis of the obtained coefficients, we have developed a Rapid Prototype of FFT based algorithm on differential protection scheme of the transformer providing the speed between 1-15 msec as compared to 100msec as per the standards of IEEE. The obtained results show that our proposed approach is rapid and could protect the power transformer from faults with accuracy.

Key-Words: - Discrete Fourier Transform, Discrete Wavelet Transform, Fast Fourier Transform, Fuzzy Logic, Inrush Current, Transformer Faults, Differential Protection

Received: April 6, 2024. Revised: September 19, 2024. Accepted: October 21, 2024. Published: December 4, 2024.

1 Introduction

The power transformers are expensive devices which need to be protected from different fault conditions. The vital objective to lessen the frequency and duration of unwanted outages puts a high pointed demand on the power transformer protective relays to operate faultlessly and impulsively [1]. The protection of power transformer has become a challenging job due to inrush and internal fault occurrence. Also there are variations in types of faults and its locations. Some of the common occurring faults are single – phase to ground fault, inter turn fault, external line to line fault, two phase to ground fault, three phase to ground fault etc [2]. Also, one of the major problems is the large magnetizing inrush current. The magnitude of which can be as high as internal fault current and may cause false tripping of the breaker [3]. A common differential relay operating on the basis of measurement and evaluation of currents at both sides of the transformer can't avoid the trip signal during inrush condition. Inrush will occur while the switching of transformer takes place and hence the circuit breaker should not trip at the time of inrush [4]. The circuit breaker, however, must trip during the fault current having the same high magnitude harmonics. Differential relay is technique is widely applied nowadays. But this technique fails to distinguish between the second frequency component of inrush current and harmonics during normal working [5]. As a result, a new relaying technique is required to differentiate between the fault and the inrush currents. Recently, to advance the conventional approaches, several new AI (artificial intelligence) features for protective relaying have been developed [6].

1.1 Inrush Phenomenon

The main problem of magnetizing inrush current is pseudo-operation of differential relay which is based on second harmonic restrain method. The inrush current also results in the damage of power transformer windings by aggregating the mechanical forces like short circuit current if remain in a high value for longer time [7]. To measure the inrush current, the secondary is kept open and the high current harmonics present in the primary side of the transformer are quantified as shown in Figure 1.1.

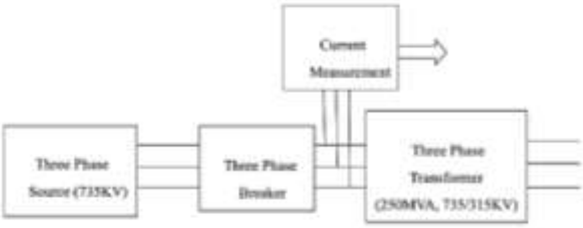

Fig 1.1.: Block diagram for inrush current measurement

1.2 Inrush Current for Amorphous and CRGO steel

The core of transformer was at first made of carbon steel but the losses were too significant. Eventually. carbon steel was replaced by silicon steel and, now, most of the power transformers uses cold rolled grain oriented silicon steel (CRGO) cores. The magnetic flux density of CRGO was found to be increased by 30% compared to the previous sheets and the magnetic saturation was decreased by 5%. Due to the demand for low core losses, low magnetostriction, the amorphous alloy cores were developed as they exhibit easy magnetization and demagnetization properties. Advantages of amorphous core are longer life, low core losses, low magnetising current, less noise, higher efficiency and less zero sequence current [8]. However, the amorphous cores were found to have higher inrush current, harmonics and higher initial cost. The saturation limit of amorphous alloy is 1.69 Tesla and for CRGO steel it is 2.03 Tesla. Hence, amorphous alloy shows better results when it is used in small size of transformers. We compared the inrush currents of both the amorphous core transformer and conventional CRGO core transformers and the results are as shown in fig. 1.2.

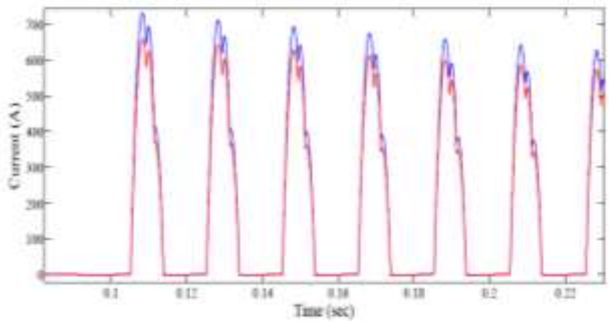

Fig 1.2.: Inrush Current for Amorphous alloy (in red) and CRGO steel (in blue)

2. Literature Survey

We focus on techniques that distinguish between inrush faults and internal faults in transformers and their protection [9-10]. Various methods were studied to incorporate the best techniques [11]-[13]. A new calculation method for transfer function (TF) comparison indices, called windowed calculation, was shown to enhance fault detection accuracy [13]. Mechanical faults in transformers, such as winding radial deformation and axial displacement, were examined using Maximal Overlap Discrete Wavelet Transform (MODWT) with Daubechies4 wavelet function for fault classification [14].

A differential protection algorithm for indirect symmetrical phase shifting transformers (ISPST) using wavelet transform (WT) and a Multi-Layer Feed Forward Neural Network (MLFFNN) was developed to classify internal faults [15]. Artificial Neural Networks (ANN) were also utilized for fault identification. Another method using hyperbolic S-transform discriminates transient fault currents and external faults [16].

Information granulation using Rough sets and cross-wavelet spectra analysis efficiently classified transformer winding faults [17]. Dissolved gas analysis was highlighted for early fault detection. A method based on differential current trajectory and weighting factors differentiated internal faults and disturbances [18].

A fast differential protection system was proposed, using differential wavelet coefficient energy to distinguish CT saturation from internal faults. Statistical indexes were used to discriminate mechanical faults, external faults, inrush currents, and internal faults [19]. Enhancements to the main differential protection principle improved fault detection sensitivity and security. The EFT, a modified discrete Fourier transform (DFT), and wavelet correlation modes were also used for fault current identification in power transformers [20].

3. DFT Analysis of Inrush Current

DFT Analysis: Fourier Transform is used to convert a signal from time domain to frequency domain. It converts each input sample to a particular frequency component. A particular frequency is assigned to each sample. Using DFT, we differentiated between the various phenomenon in our case and analyzed them [21]-[22]. We have taken one cycle (20ms) of the inrush current.

3.1 DFT Analysis of Inrush Current in Silicon Steel and Amorphous Core

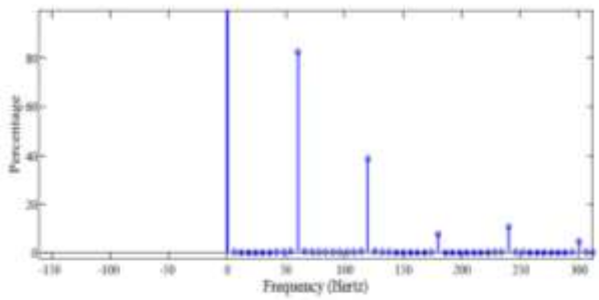

Figure 3.1.1: FFT Analysis of Inrush Current of Amorphous Core

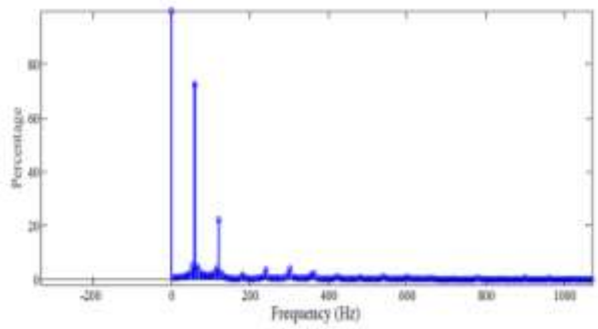

Figure 3.1.2: FFT Analysis of Inrush Current of Silicon Steel

Fundamental Frequency: 0 Hz
2nd Harmonic: 100 Hz
2nd Harmonic Content for Amorphous Core: 36%
2nd Harmonic Content for Silicon Steel: 23%

By analyzing the above values, we can conclude that second harmonic percentage for amorphous alloy is greater than that for silicon steel.

3.2 Analysis of Inrush Current for Different Phases

Phase A (2nd Harmonic Content = 36%)

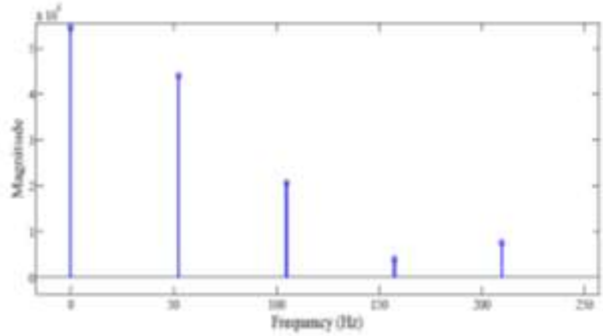

Figure 3.2.1.: FFT analysis of phase A

Phase B (2nd Harmonic Content = 73.5%)

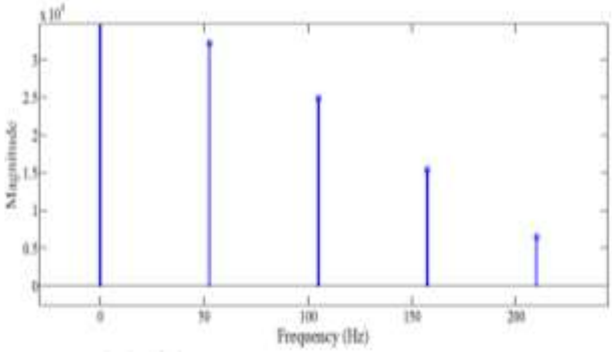

Figure 3.2.2.: FFT analysis of Phase B

Phase C (Second Harmonic Content = 78.4%)

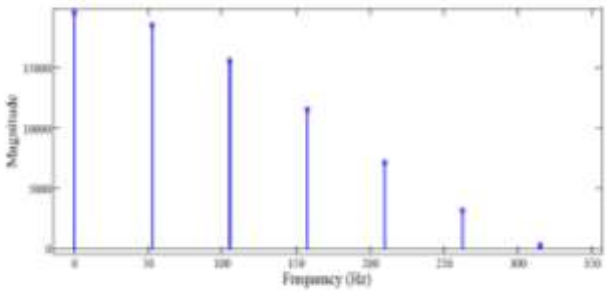

Figure 3.2.3.: FFT analysis of phase C

3.3 FFT Analysis of Internal Fault Current for Single Line to Ground Fault

For the analysis of the internal fault current, one cycle from the original signal is extracted. After extracting the internal fault signal, the FFT analysis is done using the MATLAB codes. For further analysis, the 2nd harmonic content in each case is observed. We have done FFT analysis of internal fault current for single line to ground fault, two line to ground fault and three line to ground fault for all the phases.

3.3.1. Single Line to Ground Fault

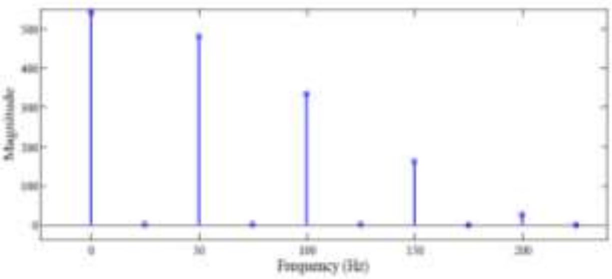

Figure 3.3.1.1.: FFT analysis of Phase A Fault (2nd Harmonic Content = 65%)

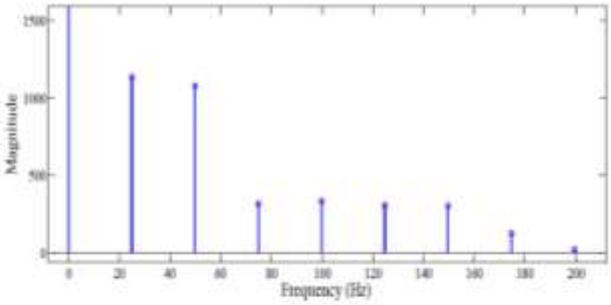

Figure 3.3.1.2: FFT analysis of Phase B Fault (2nd Harmonic Content = 24%)

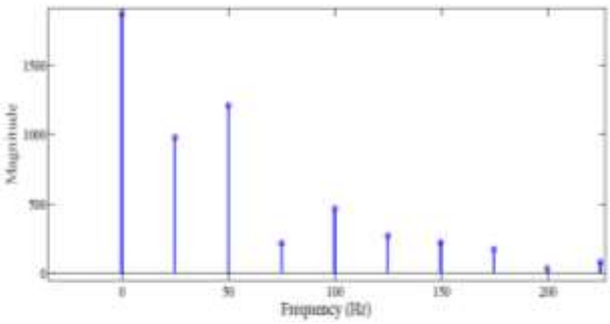

Figure 3.3.1.3: FFT analysis of Phase C Fault (2nd Harmonic Content = 25%)

3.3.2 Analysis of External Fault Current

For the analysis of the external fault current, one cycle from the original signal is extracted. After extracting the external fault signal, the FFT analysis is done using the MATLAB codes. For further analysis, the 2nd harmonic content in each case is observed. We have done FFT analysis of external fault current for single line to ground fault, two line to ground fault and three line to ground fault.

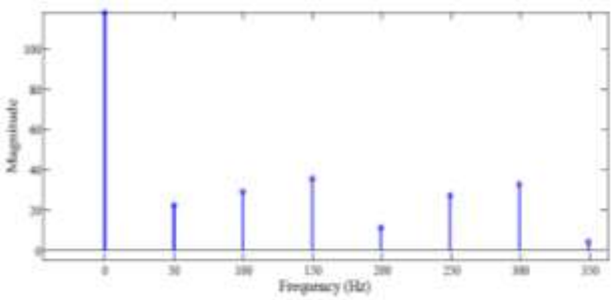

Figure 3.3.2.1.: FFT analysis of Single Line to Ground fault (2nd Harmonic Content = 22.50%)

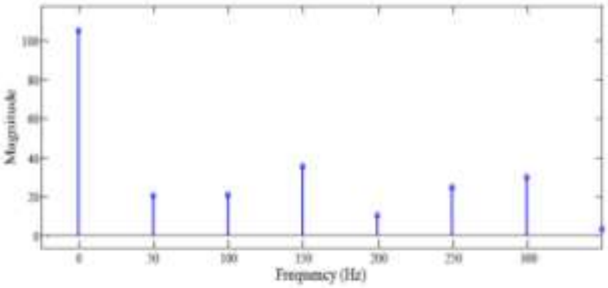

Figure 3.3.2.2.: FFT analysis of Two Line to Ground fault (2nd Harmonic Content = 21%)

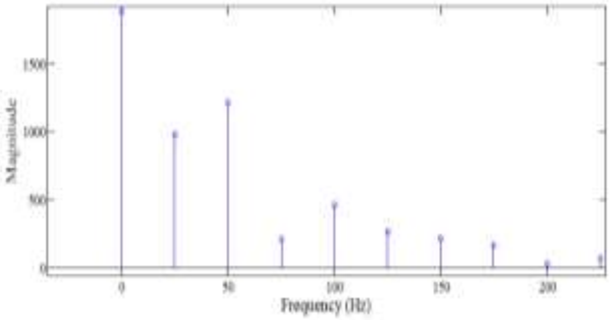

Figure 3.3.2.3.: FFT analysis of Three Line to Ground fault (2nd Harmonic Content = 24.8%)

4. Discrete Wavelet Transform Analysis of Inrush Current

The wavelet transform is also used for detailed analysis of various power transformer transients. The analysis is carried for 5 levels and different parameters are recorded for further analysis.

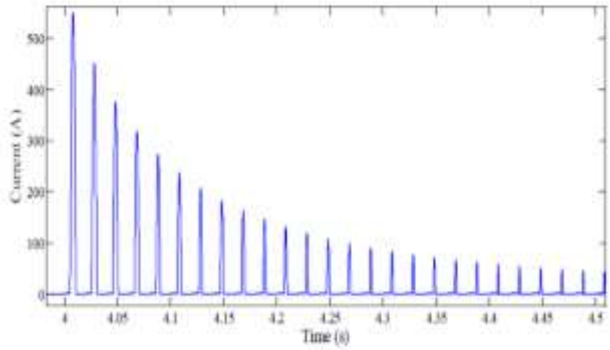

Fig 4.1: Inrush Current original signal

From the signal in Figure 4.1, the signal of the length of 20 ms is extracted and then DWT is performed up to level 5.

4.1 DWT Analysis of Inrush Current

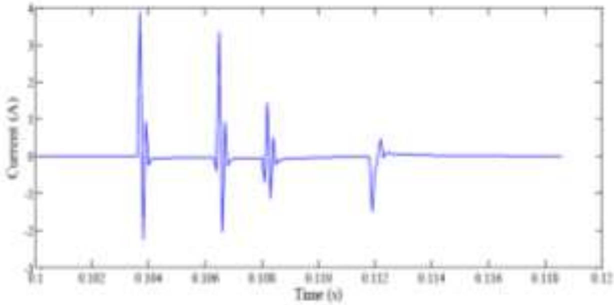

Fig 4.2: DWT analysis at level 1 decomposition

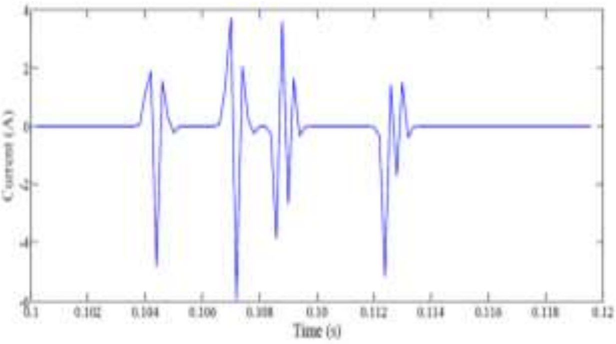

Fig 4.3: DWT analysis at level 2 decomposition

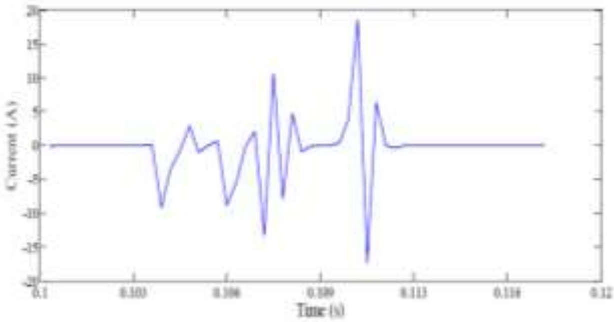

Fig 4.4: DWT analysis at level 3 decomposition

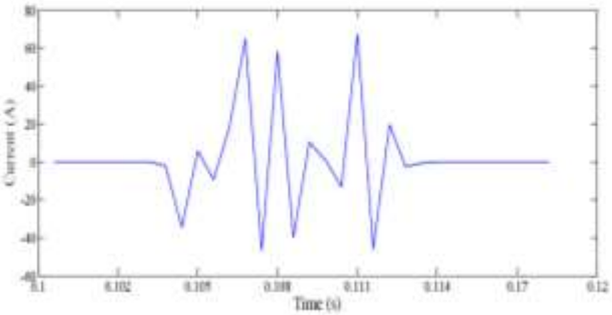

Fig 4.5: DWT analysis at level 4 decomposition

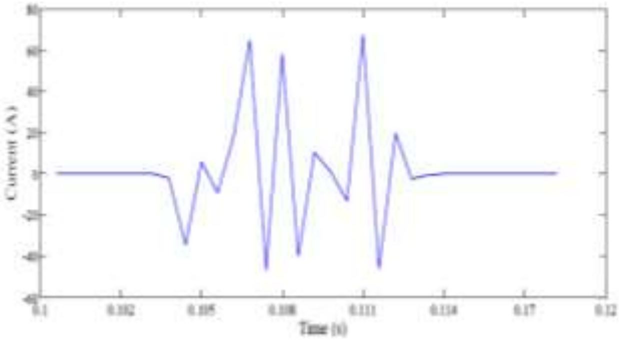

Fig 4.6: Wavelet analysis at level 5 decomposition

Frequency Band of different detailed coefficients

- Level 1 : 5 KHz – 2.5 KHz
- Level 2 : 2.5 KHz – 1.25 KHz
- Level 3 : 1.25 KHz – 0.625 KHz
- Level 4 : 0.625 KHz – 0.3125 KHz
- Level 5 : 0.3125 KHz – 0.15625 KHz

5. DWT Analysis of Internal Fault Current

In the DWT analysis of internal fault current transient, we have extracted the one cycle of 20 ms from the original signal and obtained the detailed coefficients. In the DWT analysis of the internal fault it can be seen that the signal has sharp spikes in the beginning but disappears rapidly as we increase the level of DWT. In case of inrush current, these spikes could be detected over a longer period.

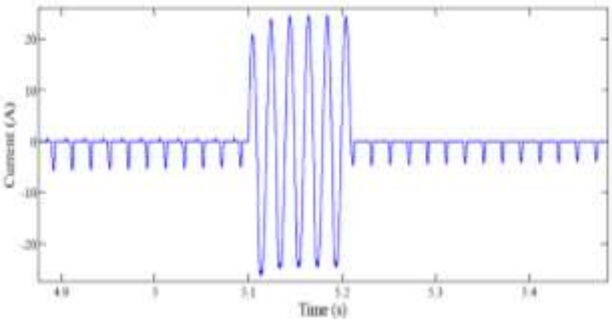

Figure 5.1.: Original signal of internal fault current

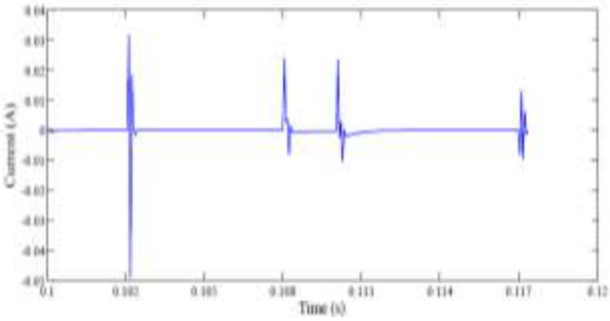

Figure 5.2.: Wavelet analysis at level 1 decomposition

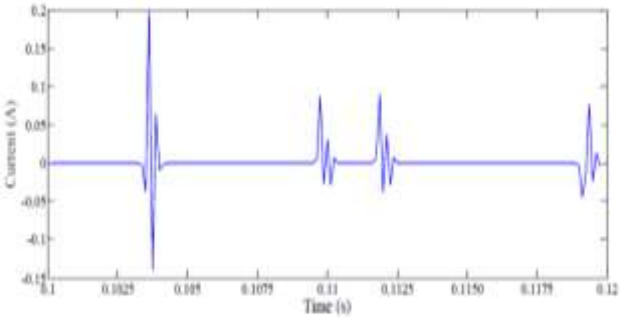

Figure 5.3.: Wavelet analysis at level 2 decomposition

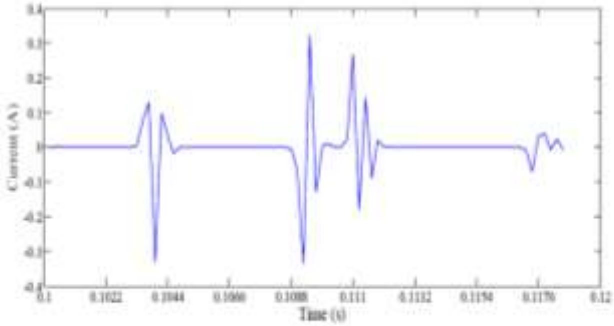

Figure 5.4.: Wavelet analysis at level 3 decomposition

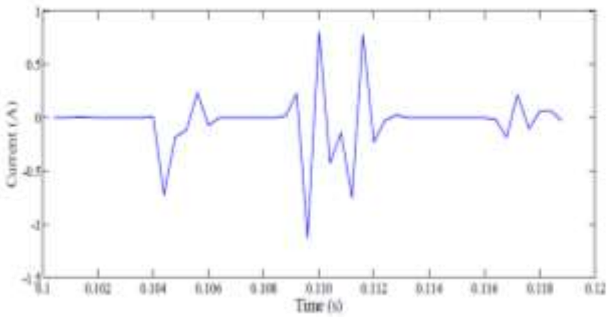

Figure 5.5: Wavelet analysis at level 4 decomposition

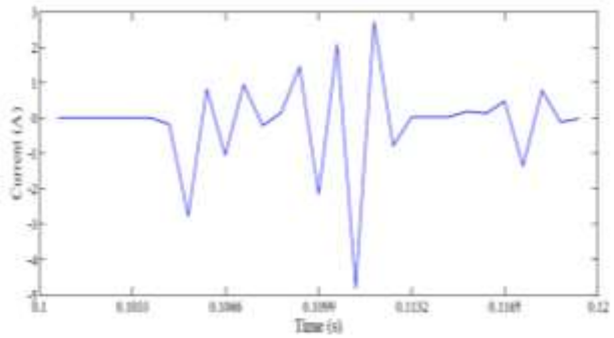

Figure 5.6.: Wavelet analysis at level 5 decomposition

After the DWT analysis of the different transients, we have extracted the maximum value of different parameters at different levels as in shown the tables 5.1. through 5.2. This data could be used in classification of faults and ultimately resulting in solving the issue of inrush current fault.

Table 5.1: Maximum value after of Inrush current's DWT Analysis

Switching Angle	Maximum Value		
Degree	Level 1	Level 2	Level 3
15°	3.19	7.37	7.96
30°	3.88	3.71	18.56
45°	2.63	8.62	18.78
60°	2.77	8.23	8.71
75°	0.69	8.53	20.92
90°	3.27	7.92	20.56
105°	1.27	4.24	11.67
120°	2.08	3.86	18.48

After the Inrush current's DWT Analysis, the maximum and minimum values at different levels are obtained. It can be observed that the maximum value is at level 3 and minimum is observed in level 1. Different values are obtained for different angles of switching on the basis of which we have made a range of the inrush current. This data is valuable for the differentiation between the faults and inrush current.

Table 5.2: Maximum value after DWT analysis of 1 line to ground fault

Switching Angle	Maximum Value		
Degree	Level 1	Level 2	Level 3
0°	0.03	0.09	0.03
30°	0.02	0.07	0.02
60°	0.03	0.06	0.03
90°	0.02	0.09	0.03
120°	0.02	0.09	0.02

6. Implementation of Fuzzy Logic for Distinguishing Between the Faults

The operation of fuzzy logic controller can be easily understood from the block diagram shown in fig 6.1. It can be seen that there are three basic blocks: input, output and the rule base. We provided three different inputs at the three different levels. These inputs are the values obtained after DWT analysis of the transients. The three inputs are Level 1, Level 2 and Level 3 detailed coefficients ranging from 0 to 500, 0 to 1200 and 0 to 2500 respectively. We have given this input to the fuzzy controller rule base where we have set up a rule set based on Mamdani model. Based on this model, the fuzzy controller distinguishes the transients into three different levels and give the data to the output block. We obtained the output in three categories external fault with range from 0 to 30, internal fault with range from 30 to 60 and inrush with range from 60 to 90.

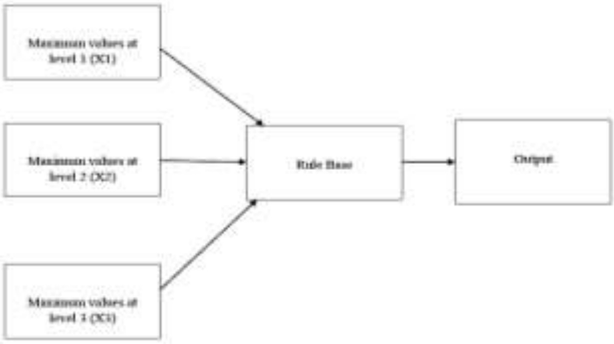

Figure 6.1: Block Diagram of Fuzzy controller

7. Digital Differential Protection System

To judge the superiority of any algorithm, the best parameters are accuracy and speed. As per the standards of IEEE, the transformer protection should be done with in 100 mSec. There are many algorithms available having 10 times the operating speed, however, in this paper, an algorithm with a speed between 1 and 15 mSec using FFT is proposed. The paper presents the simulated version of the proposed relay. The proposed algorithm identifies the harmonic content in the magnetizing current and the normal current and accordingly initiating the protective action. FFT the signal is decomposed as a set of Sine and Cosine terms given by:

$$f(t) = 0.5\, a_0 + \sum_{k=1}^{\infty} (c_k \cos \mathrm{kwt} + s_k \sin \mathrm{kwt})$$

Where a0, Ck, Sk are the dc, Sine and Cosine coefficients defined as:

$$\mathrm{Ck} = 2/N + \sum_{n=1}^{N-1} Xn \cos(2kwt/N)$$

$$\mathrm{Sk} = 2/N + \sum_{n=1}^{N-1} Xn \sin(2kwt/N)$$

The harmonic coefficients are given by :

$$F_k = C_k + S_k$$

Where: F_k is the K^{th} harmonic coefficient for k = 1, 2, ..., N x(n) and is the signal f (t) in its discrete form.

For the calculation of data, Mod / Id1 – Id2/ = 1, then inrush or internal fault, if Mod / Id1 – Id2/ = 0 then an external fault is detected. For a value of 0.3 to 0.6 of the fundamental second harmonic, the inrush current is identified and logic goes to 0 otherwise logic takes 1 indicating an external fault. More precisely, (0, 1) indicates external fault and (1,0) for magnetizing inrush current and (0,0) the calculation is reset to step 2.

This implementation is done using MATLAB/Simulink. The simulated power system built in MATLAB/Simulink is shown in Figure 7.1 in which a three phase, 250MVA, 60Hz, (735/315) kV, Y/Δ power transformer is used. The designed Conventional differential relay consists of two input portals I_{d1} and I_{d2}, and two output currents C_{T1} and C_{T2} respectively. These two input signals are divided into three parallel paths as shown. The first path leads to the Amplitude comparator. The second path modify the signal to be impressed in the harmonic test and send the result to a Harmonic comparator.

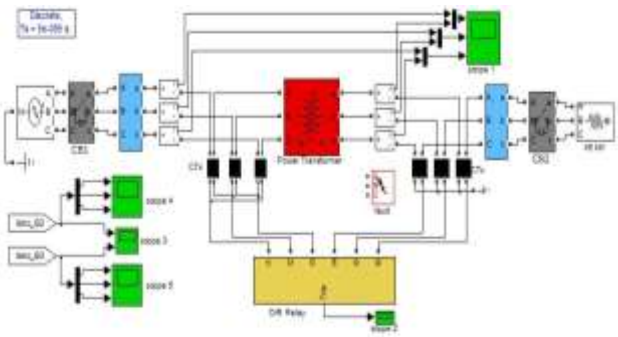

Figure 7.1: MATLAB/Simulink Model of the Proposed System

8. Simulation Results

The results are obtained for different cases:

Case 1: No load condition- Magnetizing inrush current

Case 2: Load condition- Magnetizing inrush with added load

Case 1: No load condition- Magnetizing inrush current

It is found that at 0.25 sec, no current flows through the power transformer to the secondary side and only the inrush current flows in the primary circuit of the power transformer as shown in Figure 8.1. The harmonic comparator in Figure 8.2 is illustrating the comparison of the 2^{nd} harmonic and the fundamental component for the magnetizing inrush current. The amplitude comparator result is shown in Figure 8.3. The harmonic calculation part indicates logic (0) as the amplitude comparator indicates that the differential current is equal to the inrush current. The amplitude comparator indicates logic (1) as both the graphs are overlapping. For this logic coordination (0,1) no trip signal is released as shown in Figure 8.4.

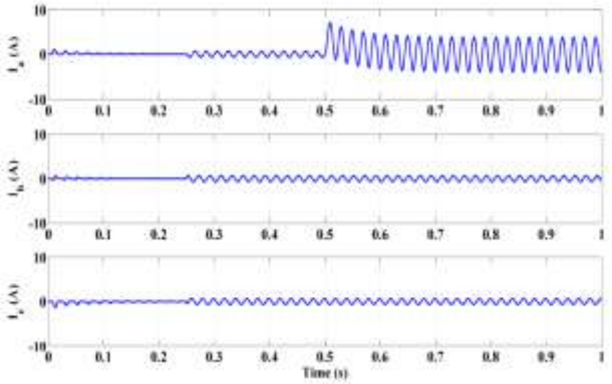

Figure 8.1: Waveforms inrush currents in the three phases of the power transformer

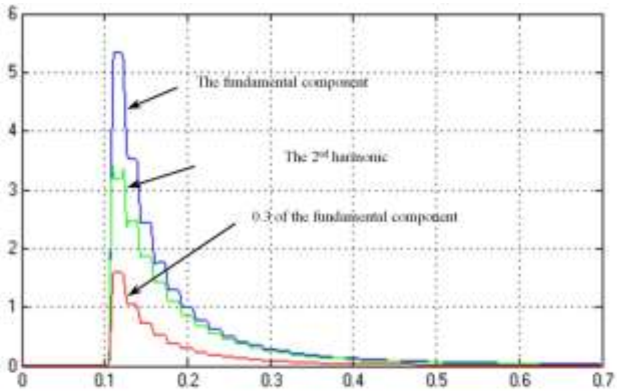

Figure 8.2: Harmonic comparator illustrating the comparison of the 2nd harmonic and the fundamental component for the magnetizing inrush current

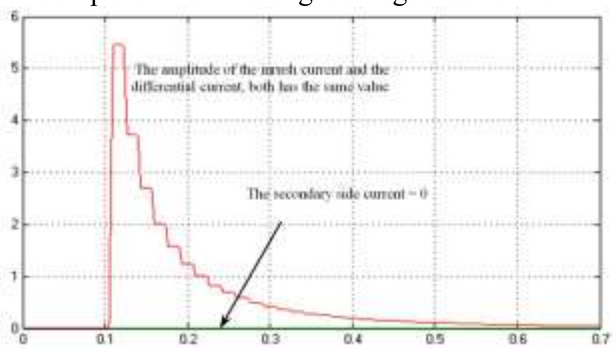

Figure 8.3. Amplitude comparator results

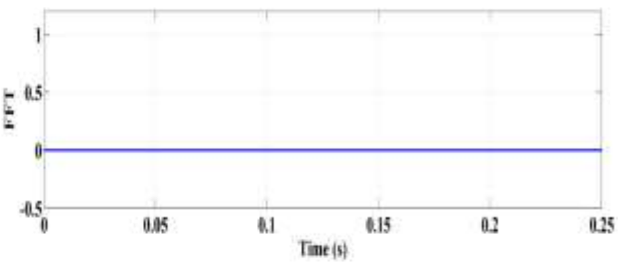

Figure 8.4: FFT-Based TRIP Signal response

Case 2: Load condition- Magnetizing inrush with added load

The CB_1 is switched on at 0.1 sec and CB_2 at 0.25 sec at the commencement of the simulation to observe the effect of load on the accuracy of the designed approach and, hence, a resistive load of 500W is added to the system at 0.25 sec. As a result, the inrush current disappears and the load current starts flowing in the transformer. However, the output currents of the primary side and secondary side of the CTs are equal as the transformation ratio of the primary and secondary CTs is properly selected, which can be obviously noticed. Figure 8.5 illustrates the load currents in the absence of inrush current. Figure 8.6 shows harmonic comparator illustrating the comparison of the 2nd harmonic and the fundamental component for the magnetizing inrush current. By harmonic comparator It is found that prior to 0.25 sec the differential current was equal to the inrush current, but with the addition of load the differential current became zero and the primary and secondary currents became equal. The amplitude comparator result is shown in Figure 8.7. The harmonic calculation part indicates logic (1) as the amplitude comparator indicates that the differential current is not equal to the inrush current. The amplitude comparator indicates logic (0) as amplitudes in both the graphs are different. For this logic coordination (1,0) no trip signal is released as shown in Figure 8.8.

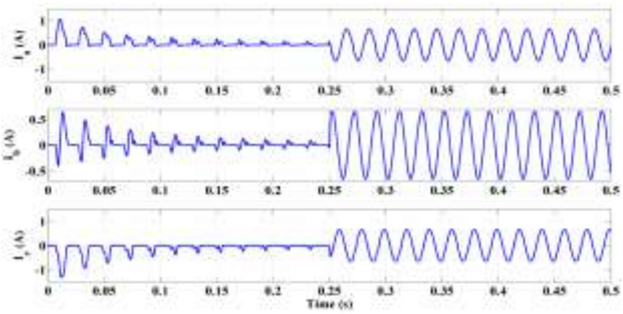

Figure 8.5: Load Current Starts flowing at 0.25 sec

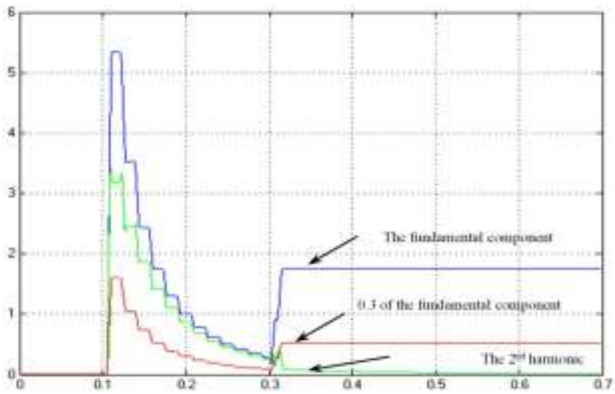

Figure 8.6: Harmonic comparator illustrating the comparison of the 2nd harmonic and the fundamental component for the magnetizing inrush current

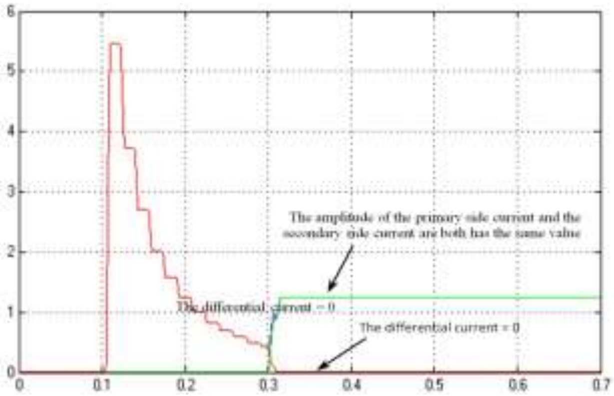

Figure 8.7. Amplitude comparator results

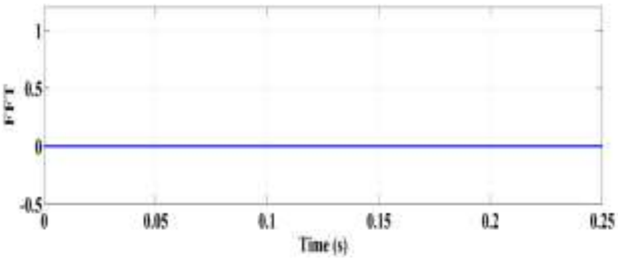

Figure 8.8: FFT-Based TRIP Signal response

8. Conclusion:

From the FFT analysis it can be concluded that the value inrush current is higher for amorphous core as compared to that of the CRGO steel. From the FFT analysis of inrush, internal and external fault, it can be observed that the 2nd harmonic content of the inrush current lies in the higher range above 50%. The 2nd harmonic content for external fault in all the cases is lying below 25%. So, the inrush and external fault transients can be easily differentiated on the basis of FFT analysis. But it is not possible to differentiate internal fault transients from inrush and external fault because the 2nd harmonic content varies from 25% to upto 70%. For this purpose, we used Wavelet Transform. In the DWT analysis, both the inrush and internal fault current is analyzed using Daubichies wavelet transform (dB – 6) up to level 5. From the DWT analysis of the internal fault, it can be observed that there are sharp spikes initially which vanishes rapidly as we increase the level of DWT. While in case of inrush current, these spikes could be observed for a longer period.

The data obtained after DFT and DWT analysis is then systematically tabulated into maximum and minimum values and given to the rule base of fuzzy logic controller. Fuzzy logic controller has been successfully implemented for the differentiation of inrush, internal and external fault using the detailed coefficients obtained by wavelet analysis. Fuzzy logic controller is found to be a very useful tool for classification of faults with minimum computational complexity.

Based on the obtained coefficients, we have developed a rapid prototype of FFT based differential protection algorithm which identifies the harmonic content in the magnetizing current and the normal current and accordingly initiating the protective action. The readings show that the trip release time is between 1-15msec which is extremely fast. The obtained results validate our claim that our proposed system is very fast and could remove the undesirable faults with accuracy.

References

[1] P. Liu, B. Jiao, P. Zhang, S. Du, J. Zhu and Y. Song, "Countermeasure to Prevent Transformer Differential Protection From False Operations," in IEEE Access, vol. 11, pp. 45950-45960, 2023
[2] J. Liu, H. Zeng, W. Niu, P. Chen, K. Xu, P. Zeng, et al., "State identification of transformer under DC bias based on wavelet singular entropy", IEEE Access, vol. 9, pp. 58944-58952, 2021.
[3] S. E. Zirka, D. Albert, Y. I. Moroz and H. Renner, "Further improvements in topological transformer model covering core saturation", IEEE Access, vol. 10, pp. 64018-64027, 2022.
[4] C. Mo, T. Y. Ji, L. L. Zhang and Q. H. Wu, "Equivalent statistics based inrush identification method for differential protection of power transformer", Electr. Power Syst. Res., vol. 203, Feb. 2022.
[5] M. Tajdinian and H. Samet, "Divergence distance based index for discriminating inrush and internal fault currents in power transformers", IEEE Trans. Ind. Electron., vol. 69, no. 5, pp. 5287-5294, May 2022.
[6] H. Samet, M. Shadaei and M. Tajdinian, "Statistical discrimination index founded on rate of change of phase angle for immunization of transformer differential protection against inrush current", Int. J. Electr. Power Energy Syst., vol. 134, Jan. 2022.
[7] A. Ashrafian, M. Rostami, G.B. Gharehpetian, “Hyperbolic S-transform-based method for classification of external faults, incipient faults, inrush currents and internal faults in power transformers”, IET Generation, Transmission & Distribution, Volume: 6, Issue: 10, October 2012
[8] D. Dey, B. Chatterjee, S. Chakravorti, “Rough-granular approach for impulse fault classification of transformers using cross-wavelet transform”, IEEE

Transactions on Dielectrics and Electrical Insulation, Volume: 15, Issue: 5, October 2008
[9] Xiong Hao, Sun Cai-xin, "Artificial Immune Network Classification Algorithm for Fault Diagnosis of Power Transformer", IEEE Transactions on Power Delivery, Volume: 22, Issue: 2, pp 930-935, April 2007
[10] Hamed Dashti, Majid Sanaye-Pasand, "Power Transformer Protection Using a Multiregion Adaptive Differential Relay", IEEE Transactions on Power Delivery, Volume: 29, Issue: 2, pp 777-785, April 2014
[11] Rodrigo Prado Medeiros, F. B. Costa, "A Wavelet-Based Transformer Differential Protection With Differential Current Transformer Saturation and Cross-Country Fault Detection", IEEE Transactions on Power Delivery, Volume: PP, Issue: 99, pp 1-1, Oct 2017
[12] Sajad Bagheri, Zahra Moravej, Gevork B. Gharehpetian, "Effect of transformer winding mechanical defects, internal and external electrical faults and inrush currents on performance of differential protection", IET Generation, Transmission & Distribution, Volume: 11, Issue: 10, pp. 2508 – 2520, 2017
[13] Lubomir Sevov, Umar Khan, Zhiying Zhang, "Enhancing Power Transformer Differential Protection to Improve Security and Dependability", IEEE Transactions on Industry Applications, Volume: 53, Issue: 3, pp 2642 – 2649, May-June 2017
[14] Senthil Kumar Murugan, Sishaj P Simon, Kinattingal Sundareswaran, "An Empirical Fourier Transform-Based Power Transformer Differential Protection", IEEE Transactions on Power Delivery, Volume: 32, Issue: 1, pp 209 – 218, Feb. 2017
[15] R. P. Medeiros, F. B. Costa, K. M. Silva, "Power Transformer Differential Protection Using the Boundary Discrete Wavelet Transform", IEEE Transactions on Power Delivery, Volume: 31, Issue: 5, pp. 2083 – 2095, Oct. 2016
[16] Daniel Guillén, Hector Esponda, Ernesto Vázquez, "Algorithm for transformer differential protection based on wavelet correlation modes", IET Generation, Transmission & Distribution, Volume: 10, Issue: 12, pp. 2871 – 2879, 2016
[17] Hadi Tarimoradi, "Novel Calculation Method of Indices to Improve Classification of Transformer Winding Fault Type, Location, and Extent", IEEE Transactions on Industrial Informatics Volume: 13, Issue: 4, pp. 1531 – 1540, Aug. 2017
[18] Sajad Bagheri, Zahra Moravej, "Classification and Discrimination among Winding Mechanical Defects, Internal and External Electrical Faults and Inrush Current of Transformer", IEEE Transactions on Industrial Informatics, Volume: PP, Issue: 99, pp 1-1, June 2017
[19] H. Z. Li, S. X. Chen, "Power transformer fault classification by combining genetic reduction with optimized multilayer support vector machine", Innovative Smart Grid Technologies - Asia (ISGT ASIA), 2015 IEEE
[20] Shailendra Kumar Bhasker, Pallav Kumar Bera, "Differential protection of indirect symmetrical phase shift transformer and internal faults classification using wavelet and ANN", TENCON 2015 - 2015 IEEE Region 10 Conference
[21] Mohd Aizam Talib, Nor Asiah Muhamad, "Fault classification in power transformer using polarization depolarization current analysis", Properties and Applications of Dielectric Materials (ICPADM), 2015 IEEE 11th International Conference
[22] Hasmat Malik, Sukumar Mishra, "Feature selection using RapidMiner and classification through probabilistic neural network for fault diagnostics of power transformer", India Conference (INDICON), 2014 Annual IEEE

Author Biography

Prof. Vikramsingh R. Parihar: He is an Assistant Professor in EE Dept., Prof Ram Meghe College of Engineering and Management, Badnera-Amravati having 13 years of experience. He has completed B.E in 2011 and M.E in 2014 from SGBAU. He is now pursuing Ph.D from RTMNU. He is editorial board member of more than 30 prestigious and recognized journals and life member of ISTE, HKSME, ICSES, IJCSE, the IRED ENZ and IAENG. His domain of research includes Digital Image Processing and Artificial Intelligence and has contributed to research in a commendable way by publishing more than 60 research papers in National/International Journals including 4 papers in IEEE Conferences. He has written 8 book chapters and also authored 6 books. He has 2 copyrights under his name. He is specialized in subjects like ECA, SS, PE, OT, AI, PCS, BEE, EMI and EM.